Article

Not peer-reviewed version

Examining the Biological Effect of 868 MHz Electromagnetic Field Emitted from Soil-Buried Antenna During the Early Stages of Development of Maize Plants

Momchil Paunov *, Boyana Angelova, Blagovest Nikolaev Atanasov, Nikolay Todorov Atanasov, Margarita Kouzmanova, Vasilij Goltsev

Posted Date: 7 May 2026

doi: 10.20944/preprints202605.0378.v1

Keywords: IoT; precision agriculture; LoRaWAN; soil sensors; RF-EMF; carrier wave; plant stress; redox status; photosynthesis; multivariate analysis

 doi:10.20944/preprints202605.0378.v1

Article

Examining the Biological Effect of 868 MHz Electromagnetic Field Emitted from Soil-Buried Antenna During the Early Stages of Development of Maize Plants

Momchil Paunov [1,*], Boyana Angelova [1], Blagovest Nikolaev Atanasov [2], Nikolay Todorov Atanasov [2], Margarita Kouzmanova [1] and Vasilij Goltsev [1]

[1] Department of Biophysics and Radiobiology, Faculty of Biology, Sofia University "St. Kliment Ohridski", 1164 Sofia, Bulgaria
[2] Department of Communication and Computer Engineering, South-West University "Neofit Rilski", 2700 Blagoevgrad, Bulgaria
* Correspondence: m_paunov@uni-sofia.bg

Abstract

IoT/LoRa devices emit radiofrequency electromagnetic fields (RF-EMF) ensuring long-range, low-power communication, and their use in precision agriculture continuously expands. Thus the interest in the impact of low intensity but long-term EMF exposure on plants has increased. In this study, maize plants were exposed to 868 MHz EMF for the first 28 days of their development with soil-buried antennas. Plants were divided into three groups: Control, Sham-exposed, and EMF-exposed. Biological effects were followed on morphological, physiological and biochemical levels every week. The plant height values were fitted to Gompertz function to model the growth. The results showed slightly faster early development of EMF-exposed plants in about 21 days. The relative dry leaf biomas from EMF-plants was a bit higher than Control and Sham until 21st day. Chlorophyll fluorescence analysis (JIP-test) indicated photosynthetic stability. Antioxidant enzymes activity, antioxidant capacity, content of malondialdehyde, hydrogen peroxide and reducing sugars were measured, and principal component analysis was done for all parameters. In general, the developmental stage accounted much more than EMF exposure for most of the observed data variation. The results suggest that under the tested conditions, IoT/LoRa-emitted EMF did not provoke adverse effects in maize and acted as a modest modulator of physiological functions.

Keywords: IoT; precision agriculture; LoRaWAN; soil sensors; RF-EMF; carrier wave; plant stress; redox status; photosynthesis; multivariate analysis

1. Introduction

Precision (smart) agriculture is the integration of modern information and communication technologies in farming in order to increase productivity, sustainability and efficient use of resources. It is based on data collection and analysis, automation, artificial intelligence and precise management methods. Data collection is carried out by wireless sensor networks based on Internet of Things (IoT) and Long Range (LoRa) protocols. LoRa works in 868 MHz and 915 MHz bands in Europe and in North America, respectively. The specific characteristics of these bands ensure long-range, low-power communication with better penetration [1]. With the increasing need for effective management of soil in changeable weather conditions, specialized antennas designed for underground deployment are being developed and tested to provide reliable communication in smart agriculture systems. Underground antennas allow for effective monitoring and management of soil and plant parameters, ensuring continuous data exchange in real time [2–4]. These technologies are beneficial for modern agriculture and guarantee more rational use of resources such as water and fertilizers,

 doi:10.20944/preprints202605.0378.v1

reduce the costs of plant growing but increase the local electromagnetic (EM) background in agricultural environments. Plants are sessile organisms permanently exposed to these artificially generated radiofrequency electromagnetic fields (RF-EMF). Even subtle physiological alterations in crop plants induced by RF-EMF could affect the quantity and quality of production.

Therefore, it is necessary to study and control the impact of RF-EMFs on plants in order to minimize potential negative effects. EMFs affect plants at different levels – from molecular to cellular and tissue, to entire organism [5]. Perception of RF-EMFs begins with absorption of energy by water molecules, alterations in their interaction with ions and in hydration of biological macromolecules, followed by changes in ion transport and enzyme activity. Very important biophysical mechanism suggested for the non-thermal effects of low intensity RF-EMF on plants involves the activation of voltage-gated calcium channels or their plant homologues, such as two-pore channels , located in the plasma membrane [6]. These channels are regulated by a highly sensitive voltage sensor. Due to high electrical resistance and low dielectric constant of plasma membrane, the effective force exerted on this sensor is strongly amplified relative to the aqueous phase [6]. The resultant channel opening triggers a rapid influx of Ca^{2+} into the cytosol, where calcium functions as a second messenger and modulates stress-responsive gene expression and downstream metabolic pathways [6–8]. Another basic mechanism of biological effects of low intensity RF-EMFs is related to alterations in enzyme activity. These initial biophysical events could provoke metabolic and proteomic alterations. Modified activity of antioxidant enzymes could lead to oxidative stress, resulting even in DNA damage.

RF-EMFs can alter the expression of genes associated with stress responses, to induce mutagenic effects, changes in the mitotic index and increased frequency of chromosomal aberrations [9–11].

All these mechanisms lead to changes at the metabolic, tissue, organ and organismal levels – changes in metabolites synthesis, root and stem length, total biomass, registered in different plant species - wheat (*Triticum aestivum* L.) lettuce (*Lactuca sativa*), *Arabidopsis thaliana* (Col.), onion (*Allium cepa),* duckweed (*Lemna minor* L.) exposed to RF-EMFs with different frequencies, intensity, time of irradiation etc. [6,9,12–14].

In tomato plants, short-term exposure to 900 MHz (5 V/m) leads to rapid expression of stress-related genes, similar to response to mechanical injury. This suggests that even weak fields can be perceived as a noxious stimulus [15].

At the whole plant level, such cellular changes may result in alterations in growth rate, biomass accumulation, root development, or reproductive performance [8,16–19]. However, the effects described in available literature reveals considerable variability: some studies report inhibitory, other – stimulatory effects, some have not obtained measurable changes in investigated parameters, especially under chronic low-intensity exposure [8,16]. The results outline a species-specific dependence of effects, determined of species-specific sensitivity, with maize (*Zea mays* L.) among the more sensitive crops [8,16]. It should be kept in mind that biological outcomes depend strongly on EMF parameters – frequency, intensity, polarization, continuous or pulsed irradiation, exposure duration etc., as well as the plant's capacity for phenotypic plasticity, which often enables adaptation to a constant low-level anthropogenic electromagnetic background [8,16].

IoT/LoRa devices operate at frequencies used in mobile telephony but at lower power densities and specific duty cycles compared to the higher-intensity sources (e.g. experimental GSM simulators) used in many earlier studies [5]. Most existing research has applied higher-power continuous exposures, and controlled studies, which included a control group and a sham exposed group and accounting for ontogenetic drift between leaf stages, are scarce. To address this gap, the present study examined the early-stage physiological responses of maize (*Zea mays* L.) – a globally important staple crop, to continuous low-power 868 MHz EMF exposure simulating IoT/LoRa carrier wave employed by soil sensors in precision agriculture. By employing a three-group experimental design (Control, Sham exposed, and EMF exposed), growth dynamics modeling, and biochemical profiling of antioxidant capacity, hydrogen peroxide (H_2O_2), MDA, enzyme activity and reducing sugars across distinct leaf ontogenetic stages, we aimed to determine whether IoT/LoRa emissions induce oxidative

 doi:10.20944/preprints202605.0378.v1

stress, disrupt carbohydrate metabolism, or alter growth rate of young maize plants under controlled conditions in laboratory.

2. Materials and Methods

Maize plants (*Zea mays* L. cultivar *Knezha-683A* from the Maize Research Institute, Knezha, Bulgaria) were grown, treated and examined in a laboratory setting. Sixteen plastic 4-liter pots were used, each containing 3 L universal peat-soil mixture with pH 6.5 (Gamma Company Ltd., Sofia, Bulgaria), which corresponded to 755±12 g dry substrate mass. 17 seeds per pot were spread homogenously and were sown at 2-3 cm depth in 16 pots. The plants were grown for 28 days in growing chambers under the following conditions:

- 80 μmol photons^{-1}m^{-2} photosynthetic photon flux density;
- 12/12 h light/dark photoperiod;
- ambient temperature and humidity in the range 25–30℃ and 55–60%, respectively.

Every few days the pots were watered properly and changed round in the chamber to minimize positional effects. The pots were divided into three experimental groups:

1. Control: Plants grown under controlled standard conditions (6 pots).
2. Sham exposed: Plants grown with antenna at the bottom of the pot buried under the soil but not emitting RF-EMF radiation in order to control for potential biological effects of antenna body presence in the pot (4 pots).
3. EMF exposed: Plants grown with antenna at the bottom of the pot buried under the soil, emitting RF-EMF (6 pots).

Flexible, low-profile antennas (2 mm thick) were designed and fabricated for the experiment. Each antenna was coated with sanitary silicone to protect against moisture when buried in soil at the bottom of a pot. The exposure setup is illustrated in Figure 1.

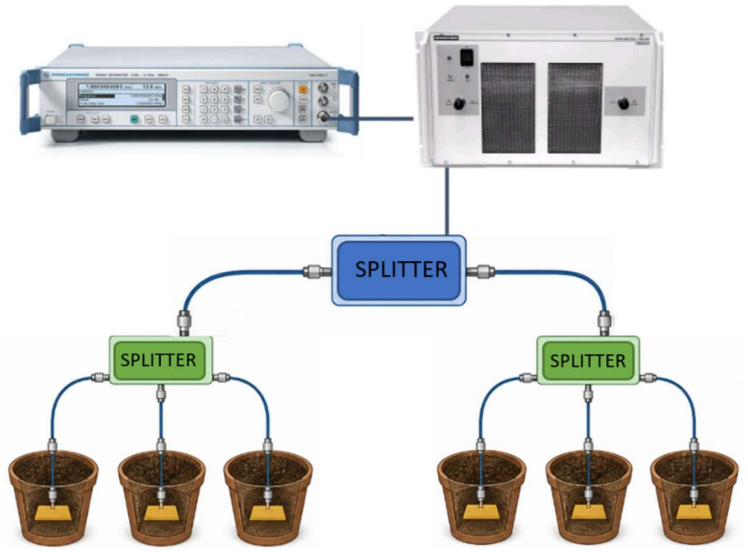

Figure 1. Exposure setup.

Each antenna placed at the bottom of a pot covered with soil was connected via a coaxial cable and an N-connector to a three-way power splitter. The two three-way splitters, connected via a two-way splitter, to the output of a power amplifier (Teseq CBA9423, 50 dB gain). The amplifier received a signal from a Rohde & Schwarz SML03 signal generator (9 kHz–3.3 GHz) at –23.8 dBm at 868 MHz. This setup delivered 10 mW input power at 868 MHz to each antenna. The chosen power of 10 mW is close to values used in precision agriculture, particularly for underground-to-above-ground communications with LoRaWAN [20].

 doi:10.20944/preprints202605.0378.v1

In addition, near the pots, measurements were performed using a spectrum analyzer under the EMF exposure conditions described above (i.e., with the generator and amplifier delivering 10 mW to each antenna buried in the soil). The results presented in Figure 2 show that the 868 MHz signal is dominant, while all other signals are at least 30–50 dB below it. Hence, we can conclude that the EMF exposure conditions are well controlled and that any observed effects would be due to the applied EMF at 868 MHz, intended to simulate LoRaWAN communications in precision agriculture.

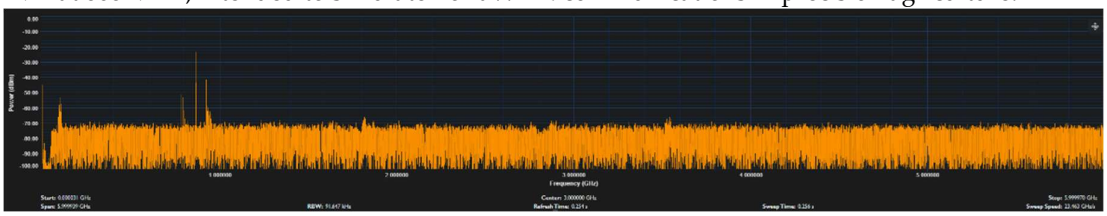

Figure 2. Measured electromagnetic spectrum in the vicinity of the pots under exposure conditions (10 mW per soil-buried antenna).

All pots were distributed between two identical growth chambers. The EMF-exposed group was placed in a separate laboratory to ensure that the control and sham groups were not subjected to significant EMF exposure. The EMF treatment was carried out throughout the 28-day experimental period covering the early stages of plant development as sprouts, seedlings and young plants, when a high sensitivity to environmental factors is expected. The exposure was interrupted once a week for short time just when analyses were performed.

The physiological state of the plants was evaluated every week by morphological, biochemical and biophysical methods. EMF exposure from a soil-buried antenna is at higher level in the roots than in the above-ground parts of a plant. Examinations of maize roots developing in soil are hardly feasible in practice because the roots are fragile, branched and intertwined, and their good separation from soil is hardly possible. So, we have focused on aerial growth and leaves analyses. Moreover, any disturbance in the root physiology would reflect on their function to provide the necessary water and nutrients to above ground parts, and would have consequences for the aerial parts, and the crop yield.

Plant growth was assessed by measuring the length of the whole plant in centimeters from the soil to the top of the longest leaf on 7^{th}, 14^{th}, 20^{th} and 27^{th} days after the seeds sowing. At the same time periods except at day 7 chlorophyll *a* fluorescence was recorded. Kinetics of chlorophyll *a* fluorescence were recorded using M-PEA fluorometer (Hansatech Instruments Ltd., UK). The performance of photosynthetic light reactions was monitored by JIP-test [21,22]. From each pot 4 plants were chosen at random excluding outliers lagging in development. From those 4 plants, 4 leaves sharing the same ordinal number from the bottom up were measured: 2^{nd} leaf for days 14 and 20, 3^{rd} leaf for day 27.

All the leaf biochemical parameters were examined on 14^{th}, 21^{st} and 28^{th} days after the seeds sowing by weighing, cutting and mixing the leaves used for fluorescence measurement for each pot. Relative dry biomass (%) was assessed as:

$$DW/FW, \quad (1)$$

where DW is dry weight and FW is fresh weight of the top parts of the investigated leaves, both measured in grams on analytical scale. The water balance was determined by calculating leaf water content (relative units) as:

$$(FW-DW)/DW\ . \quad (2)$$

Fresh weight of the mixed-cut-leaves material sampled for a particular biochemical analyses was measured separately and its dry weight was calculated utilizing (1) as:

$$DW_{biochemistry} = FW_{biochemistry} * (DW/FW). \quad (3)$$

 doi:10.20944/preprints202605.0378.v1

Plant primary metabolism was probed by the reducing sugars content versus glucose standard (mg Glucose/g DW) by the method of Plummer [23]. The redox status of the leaves was estimated by hydrogen peroxide (H_2O_2, nmol/g DW), malondialdehyde (MDA nmol/g DW), total antioxidants' content and antioxidant enzymes' activity. H_2O_2 and malondialdehyde MDA were determined following the Rainbow protocol [24]. Antioxidant capacity (μmol Trolox/g DW) was established versus Trolox standard (Trolox equivalent antioxidant capacity, TEAC) by utilizing the ABTS radical cation decolourization assay [25] as described in Kouzmanova et.al. [26]. Catalase (CAT) activity was determined by the spectrophotometric method of Aebi measuring H_2O_2 decomposition at 240 nm [27]. Superoxide dismutase (SOD) activity was assayed by SOD Assay Kit, 19160, Sigma-Aldrich [28].

The experimental results are presented as mean ± standard error of mean (SEM) values summarized at the pot level for treatment variant for each time period (day). Statistically significant differences were determined by one-way (factor: treatment) or two-way (factors: treatment and time) ANOVA followed by Duncan's new multiple range test at $p < 0.05$. All data but CAT dataset passed normality and homogeneity of variances tests. Since the discrepancy was not vast ANOVA was still applied for CAT data. However, the 6th Control pot values for the last time point (day 28) were discarded *a priory* as a spurious outlier. All the above mentioned statistic procedures along with the plotting of figures were done in R [29]. Principal component analysis of the whole data set (each data point – parameter value for a pot on a day) was performed by prcomp function in a custom R script. All variables were standardized (z-score) prior to analysis.

To characterize treatment-dependent growth trajectories, plant height data were analysed using the Gompertz model, a non-linear sigmoidal function commonly applied to plant growth processes. The model was fitted from day 7 onward, with sampling day as the predictor and plant height as the response variable. The Gompertz model was defined as:

$$h(t) = A \exp[-B \exp(-kt)], \quad (4)$$

where h(t) is plant height (cm) at time t (day), A is the asymptotic (maximal) height (cm), B is a scaling constant and k is growth-rate constant (day^{-1}). Inflection point (day), which is an indicator of the timing of maximal relative growth was also extracted from the model. Representative treatment-level fits were obtained using the complete set of observed measurements for each treatment. To assess variability in the model parameters among experimental units, the Gompertz model was also fitted separately to pot-level mean values across sampling days. Parameter estimation was performed by non-linear least-squares fitting.

Generative artificial intelligence Kimi K2.6 (Moonshot AI) and Genspark AI Assistant were used to assist in interpreting the statistical results, including performing plant growth modeling generating Figure 3b and data for Table 1, drafting and restructuring the Discussion and Conclusions sections, and harmonizing the academic style and language. All data analysis, modelling decisions, and scientific interpretations were performed by the authors, who reviewed, edited, and take full responsibility for the final content.

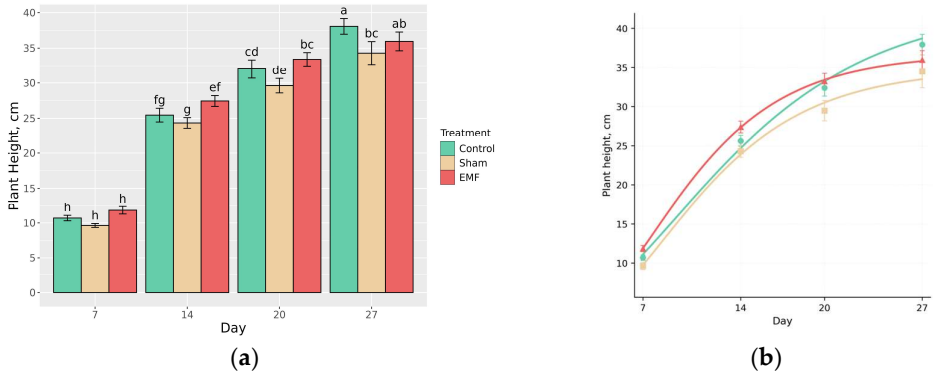

(**a**) (**b**)

Figure 3. Growth of *Z. mays* plants at normal laboratory conditions (Control), with not working antenna buried in the soil (Sham), and irradiated with 868 MHz EM wave emitted from soil-buried antenna (EMF) for 7, 14, 20 and 27 days after sowing: (**a**) Plant height (cm). Presented values are mean

 doi:10.20944/preprints202605.0378.v1

± SEM. Distinct letters denote statistically different experimental variants (two-way ANOVA, Duncan's MRT, $p < 0.05$); (**b**) Gompertz growth curves representative for each treatment group fitted to the observed plant-height data from Day 7 onward. Points represent observed mean ± SEM values for each treatment, shown with different symbols, and lines represent fitted Gompertz trajectories. Colors are shared across panels and correspond to the three treatment variants.

Table 1. Gompertz growth model parameters.

Variant	Asymptotic height, cm *	Inflection point, day *	Growth rate constant, day^{-1} *
Control	41.11±1.9 ^{a}	8.9±0.51 ^{a}	0.16±0.02 ^{a}
Sham	35.84±1.98 ^{a}	8.61±0.41 ^{a}	0.17±0.02 ^{a}
EMF	37.6±1.63 ^{a}	7.86±0.36 ^{a}	0.2±0.03 ^{a}

* Presented values are mean ± SEM. Same letters denote means that are not significantly different (one-way ANOVA, Duncan's MRT, $p < 0.05$).

3. Results

Multiple morphological, physiological, biophysical and biochemical characteristics were monitored throughout the first month (28 days) of vegetative growth to examine the scope and nature of the putative biological effect of 868 MHz EMF employed by LoRaWAN precision agriculture devices during the early stages of development of maize crop. All experimental results are described in detail below.

3.1. Morphology Analyses

Plant height increased steadily in all treatment groups throughout the experiment (Figure 3a). Mean values rose from around 10 cm on day 7 to around 35 cm on day 27 after sowing. The growth was fastest in the period between the 7th and the 14th day when height was more than doubled. Sham-exposed plants displayed the lowest mean values for each time point while EMF were the tallest at each but on the last day. However, the discrepancy between Control and Sham increased steadily to become significant on the 27th day but EMF-treated plants stayed in the Control confidence interval.

The Gompertz function was used to best model the growth of the treatment groups (Figure 3b). Overall, growth followed a largely common developmental trajectory across treatments. That is best underscored in the parameter summary presented in Table 1. The model yielded the highest growth-rate constant for the EMF group, followed by the Sham and Control groups. The estimated inflection point was likewise earliest in the EMF treatment, followed by the Sham and Control treatments. Even so, the highest asymptotic height was estimated for the Control group, indicating that the slightly faster early trajectory under EMF did not result in greater final plant size. However, all those differences were not statistically significant.

Dry leaf biomass as a percentage of fresh weight was much less dependent on time than growth alternating in the range 8-10% (Figure 4a). Only Sham exposed plants exhibited full-term dynamics – DW/FW dipped on the 21st day but on the 28th day recovered to the level on the 7th day, suggesting a transient negative effect of the antenna presence in the soil on the plants. Control experienced an increase just at the last time point. Although EMF kept its relative dry weight unchanged throughout the experiment, it had (pronounced tendencies for) higher values before reaching the last day. That fact is reminiscent of the growth dynamics. However, it should be noted that leaf analyses on the last experimental day (28th) included the 3rd leaf of the maize plants instead of the 2nd leaf as used at the previous two periods (days 14 and 21) because of its advanced senescence on the 28th day. That fact might help to better interpret the observed treatment effect discrepancies between examination days. Differences among treatment groups were most pronounced on day 21 when the 2nd leaf is 1.5 times older than at the previous period, approaching the late phase of its life. The leaf's nonoptimal physiological state should make it much more susceptible to various stress factors and thus reveal the effect of Sham exposure on the relative dry biomass.

 doi:10.20944/preprints202605.0378.v1

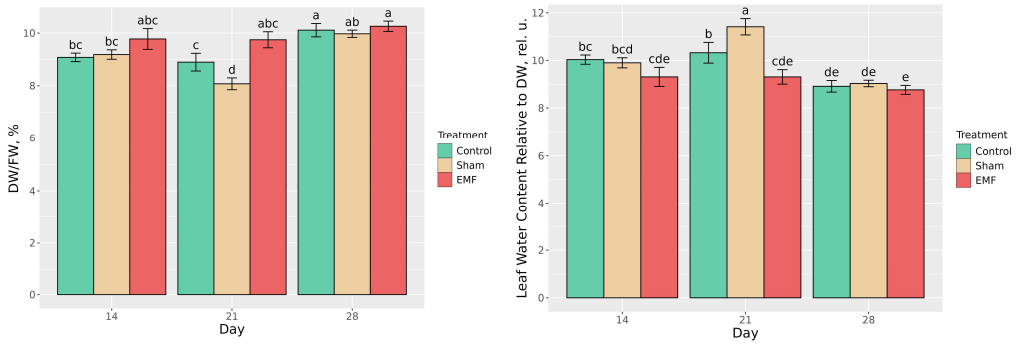

(**a**) (**b**)

Figure 4. Leaf biomass of *Z. mays* plants grown at Control conditions, Sham exposed, and exposed to 868 MHz EMF emitting from soil-buried antennas for 14, 21 and 28 days after sowing:. (**a**) Relative dry biomass (DW/FW, %); (**b**) Water content relative to DW. Presented values are mean ± SEM. Distinct letters denote statistically different experimental variants (two-way ANOVA, Duncan's MRT, $p < 0.05$).

The leaf water content (relative to DW) follows the pattern of DW/FW but in a reverse direction because both parameters are reciprocally related (Figure 4 a and b). We present both of them to highlight that relative biomass changes could be influenced by metabolic changes and/or disturbances of the water balance, while absolute biomass measurements are prone to high variability pertaining to many factors concerning the individual plant. EMF radiation seems to exert influence on relative water content leading to a mild deficit in aging leaves as noted by the significant differences between EMF and Control variants at day 21st when the measured 2nd leaf experience active senescence. At the same time point, Sham exhibited the highest water content indicating improved leaf water balance. It did not change neither with treatment nor with time for/between day 14 and 28 when measured leaves had lower physiological age, except for Control between the two time periods. However, due to the observed discrepancies in the water content, all the biochemical markers were expressed per gram leaf DW (Equation 3).

3.2. *Primary Metabolism Evaluation*

To explain morphological alterations primary leaf metabolism, i.e. photosynthesis, was evaluated by content of reducing sugars as end products of the process, and performance of the light reactions. Reducing sugars did not differ among treatment groups per day (Figure 5a). Sugars decreased with time for all variants but EMF – more strongly for Control than Sham.

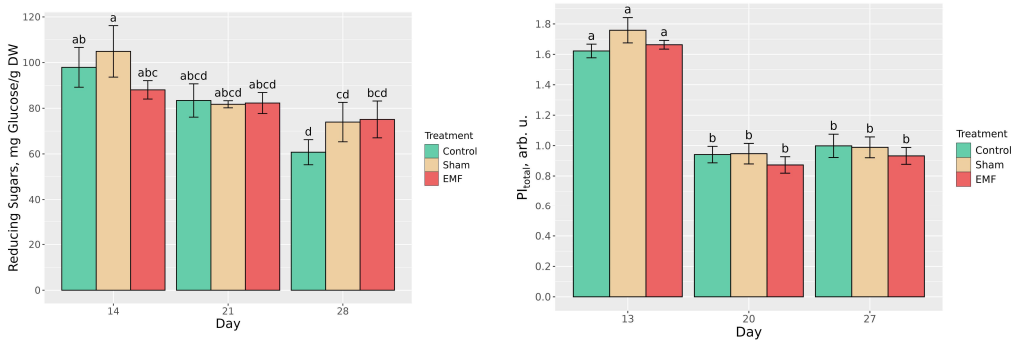

(**a**) (**b**)

Figure 5. Primary metabolism markers in *Z. mays* leaves for Control, Sham and 868 MHz EMF-irradiated plants at 14, 21 and 28 days of treatment: (**a**) Reducing sugars content (mg Glucose/g DW); (**b**) Performance index of the total light-dependent photosynthetic reactions (PI_{total}). Presented values

 doi:10.20944/preprints202605.0378.v1

are mean ± SEM. Distinct letters denote statistically different experimental variants (two-way ANOVA, Duncan's MRT, $p < 0.05$).

The performance index of the total photosynthetic light-phase (PI_{total}) probed by JIP-test did not depend on treatment but dropped heavily on the 20th day to stable levels (Figure 5b). This parameter integrates the concerted action of light absorption, primary photochemistry, electron transport and production of NADPH (and ATP) in thylakoid membranes. The fluorescence data supported a picture of overall functional stability of the photosynthetic machinery that is consistent with the morphological layer, where time progression also dominated over treatment in determining the final phenotype. Moreover, the clear time-dependent decrease of reducing sugars and PI_{total} and the lack of differences between 20(21) versus 27(28) days might underline the determining influence of whole-plant metabolism shifts during the development and not a leaf age dependence.

3.3. Redox Status Examination

As further step in seeking 868 MHz EMF-related effect the leaf redox status was investigated. Malondialdehyde, a marker of lipid peroxidation, was determined to explore the possibility of treatment-related oxidative stress (Figure 6). However, actual lipid damage correlated to treatment was not found. On the contrary, transient dynamic alterations in the opposite direction, i.e. lowering the oxidation level, were revealed. EMF exposed plants displayed lower MDA content on the 21st day of growth and returned to initial levels at the end of the experiment. Similar but insignificant alterations on the midterm were present for Control but for Sham such was not practically present.

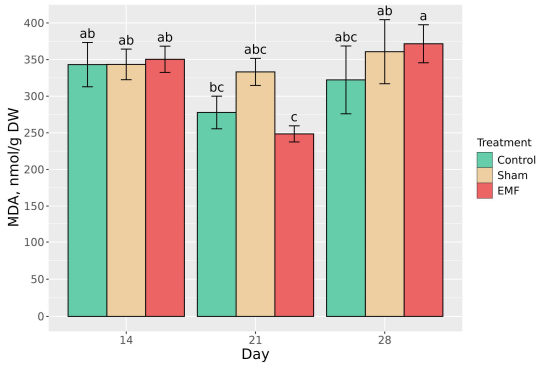

Figure 6. Malondialdehyde (MDA, nmol/g DW) in leaves of Control, Sham and 868 MHz EMF-treated for 14, 21 and 28 days *Z. mays* plants. Presented values are mean ± SEM. Distinct letters denote statistically different experimental variants (two-way ANOVA, Duncan's MRT, $p < 0.05$).

Since oxidative stress is determined by the imbalance of oxidants versus antioxidants in favor of the former both chemical species were measured in the leaves. The hydrogen peroxide was measured as an (pro-)oxidant giving the most dangerous reactive oxygen species (ROS) *in vivo* – hydroxyl radical (·OH). H_2O_2 displayed clear time but no treatment dependence (Figure 7a). H_2O_2 is generated in all aerobic cells due to the vast presence of the best oxidant in biology – the molecular dioxygen, and its ability to extract single electrons from organic molecules resulting in superoxide radical ($\cdot O_2^-$), at first and consequently in H_2O_2. Hence such strong linear dynamics might indicate diminishing metabolic activity during the vegetative period independent on EMF or Sham conditions and reminds of the less pronounced time-trend for reducing sugars.

 doi:10.20944/preprints202605.0378.v1

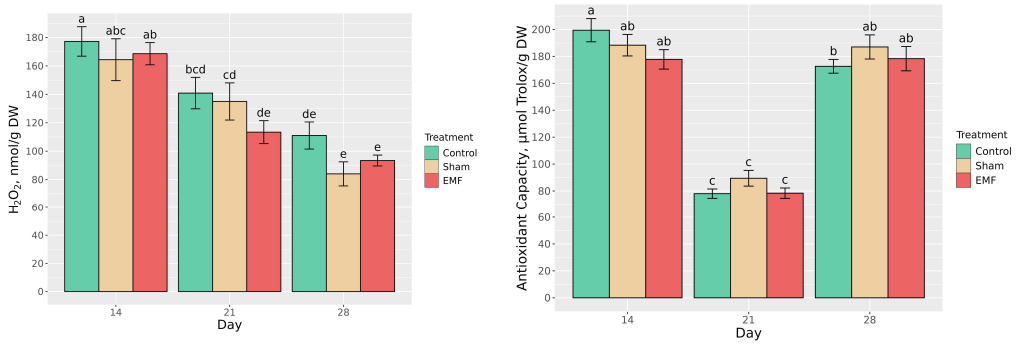

Figure 7. Redox status of *Z. mays* leaves for Control, Sham and 868 MHz EMF-exposed variants at 14, 21 and 28 days of treatment: (**a**) Hydrogen peroxide quantity (H_2O_2, nmol/g DW); (**b**) Total antioxidant capacity (µmol Trolox/g DW). Presented values are mean ± SEM. Distinct letters denote statistically different experimental variants (two-way ANOVA, Duncan's MRT, $p < 0.05$).

The antioxidants were determined by Trolox equivalent antioxidant capacity (TEAC) of the leaf extracts (Figure 7b). Once again, EMF or Sham exposure did not influence the parameter. On the other side, there was two-fold decrease in TEAC on the 21st day while the values at the other periods were identical pointing to the leaf physiological age as the determinant of the antioxidant content.

H_2O_2 is not just a byproduct of the aerobic metabolism. It is an important messenger molecule in the cell involved in many signal pathways, so its concentration is tightly regulated by its enzymatic production and degradation. The activity of superoxide dismutase (SOD) – the enzyme that generate H_2O_2 is shown in Figure 8a. The pattern in this figure highly resembles that of H_2O_2 which is to be expected – plant age-related physiology changes were the main factor in determining SOD activity. Surprisingly, some effect of 868 MHz EMF on SOD was revealed: the treatment lowered moderately its activity compared to Control/Sham at day 14 and – just to Sham at day 21 but not at the last period.

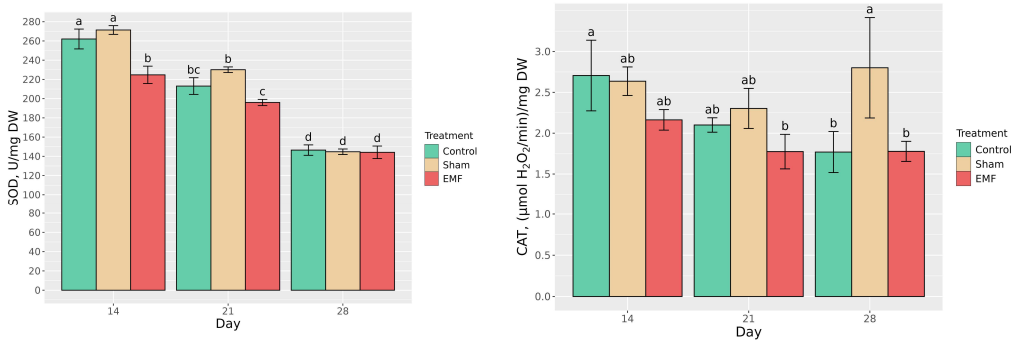

Figure 8. Antioxidant enzymes in *Z. mays* leaves from Control, Sham and 868 MHz EMF-exposed plants at 14, 21 and 28 days of treatment: (**a**) Superoxide dismutase (SOD) activity (U/mg DW); (**b**) Catalase (CAT) activity, (µmol H_2O_2/min)/mg DW. Presented values are mean ± SEM. Distinct letters denote statistically different experimental variants (two-way ANOVA, Duncan's MRT, $p < 0.05$).

The activity of catalase (CAT) – the main enzyme degrading H_2O_2, expressed much weaker dynamics than SOD, significant for the Control only where it decreased from the first to the last time point (Figure 8b). Moreover, Sham on the 28th day was the only variant to significant deviate from the treatment groups in a time point. Tendency for lower values for EMF was noticed.

 doi:10.20944/preprints202605.0378.v1

3.4. Multivariate Analysis

Principal component analysis (PCA) of the full biochemical, physiological and morphological dataset revealed that variation was structured primarily by developmental stage, with treatment-related displacement superimposed as a secondary pattern (Figure 9). The first three components explained 73.1% of the total variance.

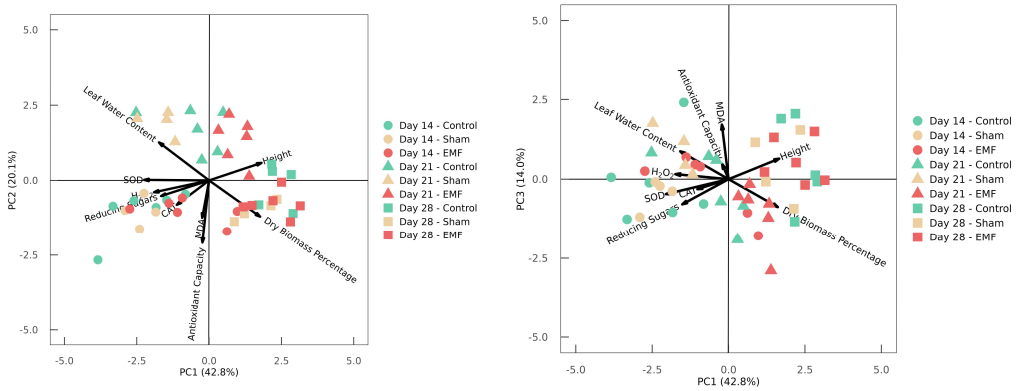

(**a**) (**b**)

Figure 9. Principal component analysis (PCA) biplot of morphological, biochemical, and physiological parameters measured in Z. mays across three treatments (Control, Sham, EMF) and three developmental stages (Day 14, Day 21, Day 28): (**a**) PC1–PC2 plane; (**b**) PC1–PC3 plane. Percentage variance explained: PC1 = 35.6%, PC2 = 20.3%, PC3 = 18.6%. Symbols represent individual pots, coded by sampling day (circles = Day 14, triangles = Day 21, squares = Day 28) and by treatment colour (green = Control, yellow = Sham, red = EMF). Variable vectors indicate the contribution of each parameter (height, dry biomass percentage, leaf water content, reducing sugars, MDA, H_2O_2, TEAC, SOD, CAT) to the principal component axes; vector length reflects the strength of contribution and orientation indicates the direction of correlation. All variables were standardized (z-score) prior to analysis. PCA was performed on the correlation matrix using the prcomp function in R.

On the PC1–PC2 plane, samples arranged along PC1 in a clear temporal sequence: Day 14 (circles) at the negative end, Day 21 (triangles) intermediate, and Day 28 (squares) toward the positive end. The variable vectors indicate that PC1 was driven by plant height and dry biomass (positive direction), opposing reducing sugars, SOD, CAT, and H_2O_2 (negative direction). This anticorrelation reflects the metabolic reallocation associated with rapid stem elongation.

Treatment effects emerged along PC2. Control samples (green) concentrated in the lower half, Sham (yellow) displaced markedly upward, and EMF (red) showed greater scatter, particularly at Day 14. By Day 28, the EMF cluster tightened, suggesting consolidation of an initially variable phenotype. The partial EMF–Sham overlap, together with their joint separation from Control, indicates that exposure context introduced a measurable physiological component without producing a distinct EMF-specific signature.

The PC1–PC3 projection corroborated the temporal gradient, while PC3 captured additional variance linked to MDA and TEAC, contributing to fine-scale separation of late-stage samples.

4. Discussion

The maize growth indicate small transient treatment-related differences (Figure 3). EMF exposure had slightly accelerated the early growth without producing a bigger plant size at the end of experiment. In the available literature EMF-related effects on plant growth vary with field characteristics, exposure regime, developmental stage, and species. EM frequencies of 900 and 1800 MHz ranges are widely investigated. Most of the studies report inhibition of early seedling growth, but stimulation or lack of measurable morphological effects were also noticed. Exposure of onion (*Allium cepa*) bulbs to 900 and 1800 MHz EMF for 0.5, 1, 2 and 4 hours affected root meristematic cells

 doi:10.20944/preprints202605.0378.v1

and reduction in root length and increase in thickness were observed. A significant increase in the mitotic index after 2 and 4 h exposure, and in chromosomal aberrations during 0.5–4 h of exposure were also observed. Authors concluded that EMFs of 900 and 1800 MHz adversely affect root meristems in onion plants and induce cytotoxic and DNA damage, more pronounced at 1800 MHz than at 900 MHz [13]. Wheat plants (*Triticum aestivum* L.) exposed to 2850 MHz also showed a reduction in root and stem length, and in total biomass. A decrease in the concentration of photosynthetic pigments and in the activity of enzymes related to carbohydrate metabolism was also found [6]. Lettuce (*Lactuca sativa*) exposed to frequencies of 1890–1900 MHz, 2.4 GHz and 5 GHz showed a significant decrease in photosynthetic efficiency under outdoor conditions, together with suppressed expression of stress-related genes and accelerated flowering [9]. Duckweed (*Lemna minor* L.) showed reduced growth when irradiated with 900 MHz (2 hours, 23 V/m), while the same radiation at 400 MHz did not lead to a significant effect. At stronger fields (390 V/m) further growth suppression was found. A significant increase in peroxidase activity was observed at 900 MHz [14]. Maize seedlings irradiated with 1800 MHz and SAR 0.169 W/kg for 0.5–4 h showed significant physiological and biochemical changes, including reduced root and coleoptile length, decrease in the content of photosynthetic pigments and total carbohydrates, as well as strongly increased activity of enzymes involved in metabolism [30]. In maize (*Zea mays*) exposed to 900 MHz, an increased germination rate was reported [31].

In a previous study we failed to register statistically significant changes in morphological (growth rate, biomass) and physiological characteristics (photosynthetic pigments, reducing sugars, anthocyanins and malondialdehyde) 10 days after 2-hour exposure of wheat and maize sprouts to 900 MHz EMF, 370 V/m, continous wave [32]. The results of our current experiment are more consistent with mild modulation of growth dynamics than with either pronounced growth promotion or growth suppression. The alterations in relative dry biomass and leaf water content support this hypothesis – the differences between exposed and control/sham exposed plants faded to the end of experiment. The absence of significant differences in final seedlings height, leaf biomass and leaf water content suggest that maize plants can adapt to EMF with investigated parameters and exposure conditions. However, interpretation of the day-28 leaf data requires explicit methodological contextualisation. During the first three weeks of vegetative growth, the second leaf served as the primary photosynthetic organ and was the subject of all analyses on days 14 and 21. By day 28, this leaf had entered advanced senescence, necessitating a transition to the third leaf, which at this chronological stage is functionally younger and physiologically less mature than the second leaf was at the preceding time points. This ontogenetic reset introduces a discontinuity in the time series: the apparent convergence of relative dry biomass and water content across treatments on day 28 (Figure 4) reflects, at least in part, the inherent juvenility of the new leaf cohort rather than a genuine dissipation of treatment effects. Consequently, the EMF-related elevation in dry biomass and the Sham-related water-balance perturbation observed at day 21 – measured on the same leaf at a comparable physiological age – represent the more reliable indicators of treatment-specific modulation. The data at day 28 contribute to treatment comparison completeness but must be weighted cautiously when inferring treatment trajectory.

The Sham condition introduced a measurable morphological signal distinct from both Control and EMF. Sham-exposed plants consistently displayed the lowest mean height values, with the divergence from Control attaining statistical significance by day 27. Furthermore, the transient depression of relative dry weight in Sham plants on day 21, followed by apparent recovery on day 28, indicates that the physical presence of the antenna in the rhizosphere was not biologically neutral. Whether through altered soil compaction, modified microhydrology, or subtle chemical effects, the inactive device functioned as a handling control rather than as a strict procedural blank – a distinction that is methodologically critical in studies of low-intensity environmental factors [5]. The fact that at the periods when Sham expressed lower than Control height and biomass EMF showed no chnages may indicate hidden protective capability of the low-power 868 MHz EM wave neutralizing negative antenna matherial influences on the roots but further detailed investigations proving those are needed to prove this hypothesis.

 doi:10.20944/preprints202605.0378.v1

The photosynthetic and metabolic data reinforce the ontogenetic dominance observed at the morphological level. The performance index of total photosynthetic light reactions (PI_{total}), probed by JIP-test, showed no treatment-dependent variation at any sampling point, indicating broad functional stability of PSII reaction centres, electron transport, and energy transduction [21,22,33]. This stability stands in contrast to reports of EMF-induced photosynthetic disruption at higher frequencies or power densities. Tang et al. demonstrated proteome-level disturbance of the photosynthetic machinery in *Microcystis aeruginosa* [7], Pal et al. reported long-term effects of 2850 MHz EMF on carbohydrate metabolism in wheat [6], and Roux et al. documented altered transcription, translation, and electric charges in tomato exposed to 900 MHz fields [34]. External RF-EMF can interfere also with the plant's endogenous electrophysiological signaling based on electric potential fluctuations, potentially disturbing intercellular communication and adaptive responses to other environmental factors [35]. Stefi at al. investigated non-thermal effects of exposure of *Arabidopsis thaliana* to 1882 MHz, 2072 V/m, 24/7 for 2, 3, or 4 weeks and found alterations in leaves development, reduction in the number of chloroplasts, decrease of stroma thylakoids and the photosynthetic pigments, resulting in a weak photosynthetic potential and a consequent reduction of the primary productivity – reduced biomass of the above the ground parts and the roots, with roots more affected [12]. The absence of comparable perturbations under the present exposure parameters suggests that 868 MHz carrier-wave emissions from soil-buried LoRaWAN antennas do not impact photosynthetic machinery.

Reducing sugars and PI_{total} declined synchronously across all treatments between days 14 and 21, followed by apparent stabilisation through day 28 (Figure 5). As with the morphological parameters, this temporal pattern must be interpreted through the lens of leaf-age discontinuity. The transition from the senescing second leaf (days 14 and 21) to the functionally younger third leaf (day 28) resets the physiological clock; the third leaf is expected to naturally retain higher photosynthetic capacity and greater soluble sugar content than its predecessor would have exhibited at the same chronological age of the plant. Thus, the plateau observed on day 28 should reflect an ontogenetic artefact rather than a metabolic recovery or treatment-specific effect. However, the clear time-dependent decrease in these parameters between days 14 and 21, and the lack of differences between the mid-term and terminal measurements could also be determined by whole-plant developmental shifts rather than leaf-age dependence *per se*.

The absence of treatment-specific differences in reducing sugar content indicates that carbon fixation and partitioning were not perturbed by EMF exposure. The metabolic reallocation associated with the transition from heterotrophic seedling growth to autotrophic establishment – wherein stored reserves are mobilised and subsequently diluted by structural biomass accumulation – proceeded identically across all treatments [36]. In this context, the insignificant Gompertz-derived acceleration in stem elongation observed for EMF plants (Table 1) cannot be attributed to enhanced photosynthetic output per unit leaf area. Rather, it suggests a more efficient utilisation or altered partitioning of fixed carbon toward structural elongation, a quantitative adjustment of sink–source relationships that remained within the homeostatic range and did not coalesce into a generalized metabolic stress response. It should be noted that reducing sugars (all the monosaccharides and many disaccharides) have many important roles in plants other than being nutrients: signalling molecules involved in stress responses and photosynthesis regulation, anti-oxidative processes, etc. Glucose, as a signalling molecule, regulates all processes of plant growth and development. Decresse of reducing sugars concentration could affect all these processes with the respective consequences to the plant.

Malondialdehyde, a widely employed proxy for lipid peroxidation [24], was not elevated in EMF-exposed plants; on the contrary, it was transiently lowered on day 21 relative to Control before returning to baseline levels by day 28 (Figure 6). This absence of treatment-related oxidative damage contrasts sharply with studies employing higher-intensity RF-EMF. Sharma et al. demonstrated that mobile phone radiation inhibited root growth in *Vigna radiata* by provoking oxidative stress, evidenced by elevated MDA and H_2O_2 levels [19], while Kumar et al. similarly linked 1800 MHz EMF-induced growth inhibition in maize to metabolic disruptions entailing redox imbalance [30]. Some authors also considered that exposure to RF-EMF in 900 MHz–1.8 GHz range acts as an abiotic stressor, inducing oxidative stress assessed by increased MDA levels and membrane damage [16,31].

 doi:10.20944/preprints202605.0378.v1

To compensate for this effect, plants upregulate antioxidant enzymes (e.g. catalase) and accumulate proline as osmoprotectant [31,37].

Hydrogen peroxide and total antioxidant capacity (TEAC) exhibited no statistically significant differences between the treatment groups but pronounced temporal dynamics: H_2O_2 steadily decreased while TEAC dropped sharply on day 21 before recovering on day 28 (Figure 7). Once again, the day-28 recovery must be interpreted with circumspection owing to the leaf-age discontinuity: the third leaf, being metabolically younger, possesses a redox profile characteristic of earlier developmental stages – higher antioxidant capacity and lower steady-state H_2O_2 – than the senescing second leaf would have displayed.

The enzymatic antioxidant profile, however, revealed a selective EMF effect that persisted independently of this confounder (Figure 8). SOD activity was moderately but significantly lower in EMF-exposed plants on day 14. Crucially, this reduction was not accompanied by significantly elevated H_2O_2 (despite the similar overall pattern between SOD and H_2O_2) or MDA, implying that diminished SOD activity reflected decreased substrate availability – i.e., reduced superoxide radical ($\cdot O_2^-$) generation – rather than compromised antioxidant defence. This interpretation aligns with the concept that low-intensity EMF may modulate mitochondrial and plasmalemmal electron leakage without imposing oxidative challenge [5]. Frequency-dependent modulation of antioxidant enzyme activity has been previosly reported supporting the plausibility of such parameter-specific adjustments [12,14].

CAT activity displayed weaker dynamics, with a non-significant tendency toward lower values in EMF plants and a notable elevation in Sham on day 28. The Sham-related deviation, statistically significant compared to Control, is particularly instructive because it was measured in the younger third leaf. The absence of a comparable Sham effect in the second leaf on days 14 and 21 suggests that the physical presence of the antenna may have induced a delayed adaptive response manifesting in the third leaf. Regardless of the particular mechanism behind such CAT activation, this divergence reinforces the conclusion that the Sham antenna was not biologically inert and should be interpreted as a handling control [5].

Collectively, the redox state data indicate that 868 MHz EMF exposure under LoRa-relevant conditions did not provoke oxidative stress in young maize. Instead, it induced a mild, quantitative adjustment of the antioxidant enzyme network superimposed on a developmentally driven redox landscape. The biochemical markers, being the most responsive analytical layer among morphology or fluorescence, captured the finest treatment-related modulation, yet these changes remained trait-specific and did not coalesce into a generalized stress syndrome. This pattern – limited parameter-specific shifts, partial overlap with Sham, and attenuation over time – is consistent with adaptive physiological tuning within the normal homeostatic range, as corroborated by the multivariate perspective discussed below.

The multivariate analysis (Figure 9) provides a consolidated view that summarizes the patterns observed at the univariate level. Across the three analytical layers – morphology, photosynthetic performance, and biochemistry – a consistent hierarchy emerged: developmental stage was the dominant source of variation, while treatment effects remained selective, trait-dependent, and context-sensitive. Such ontogenetic dominance over stress-related modulation is frequently observed in crop physiological studies employing integrated phenotyping approaches , where the maturational programme sets the baseline against which environmental perturbations are superimposed [5,38].

The PCA revealed that the first principal component captured primarily the ontogenetic trajectory, with plant height and biomass driving the positive pole and metabolite pools (reducing sugars, antioxidant enzymes, H_2O_2) loading in the opposite direction. This axis thus encapsulates the fundamental physiological trade-off between structural growth and metabolic maintenance that characterizes early vegetative development in maize [36]. Against this strong developmental background, treatment-related displacement was expressed mainly along PC2 and, to a lesser extent, PC3.

 doi:10.20944/preprints202605.0378.v1

The upward shift of Sham samples along PC2, distinct from the Control cluster below, indicates that the physical presence of the antenna introduced a measurable multivariate signal even in the absence of active electromagnetic emission. This observation is methodologically important: it demonstrates that the exposure device itself – whether through subtle microclimatic effects, mechanical proximity, or other non-EMF cues – was not biologically neutral. Consequently, the Sham condition should be interpreted as a handling control rather than as a strict procedural blank, a distinction that has been emphasized in studies of low-intensity physical factors in plant biology [5].

The EMF group occupied an intermediate position, overlapping partially with Sham yet exhibiting greater dispersion, particularly at Day 14. This scatter reflects the interplay of two concurrent processes: inherent biological heterogeneity, evident across all treatments and consistent with the natural variability documented in replicated plant physiological experiments [39], and treatment-induced phenotypic plasticity, whereby the physiological profile adjusted to the specific exposure context [40]. The concept of phenotypic plasticity as an adaptive mechanism allowing plants to cope with environmental heterogeneity is well established, and its expression under chronic low-intensity stressors has been reported in several crop species [41,42]. The consolidation of EMF samples into a tighter cluster by Day 28 suggests that early-stage plasticity gradually attenuated as development progressed, possibly because the plants either acclimated to the chronic low-level exposure or because the developmental programme itself increasingly constrained the range of permissible physiological states.

The multivariate pattern supports the interpretation that EMF exposure acted as a mild modulator rather than as a deterministic stressor. Had the electromagnetic field imposed severe physiological disruption, one would expect a coordinated displacement across multiple parameters – a generalized stress syndrome visible as a distinct, treatment-specific cluster in the PC space. Instead, the PCA serves as an integrative confirmation that EMF exposure in maize, under the tested conditions, is one of quantitative physiological adjustment superimposed on developmental progression, rather than qualitative reorganization indicative of physiological impairment [17]. Similar modulatory effects of low-power EMF on plant antioxidant and metabolic status, without evidence of adverse physiological effects, have been described in maize and other crops under smart-agriculture-relevant exposure scenarios [5].

5. Conclusions

The present study examined the biological effects of 868 MHz electromagnetic fields, emitted from soil-buried antennas under conditions representative of IoT/LoRaWAN precision agriculture deployments, on young maize plants during the first 28 days of vegetative development. Under the present experimental conditions, maize plants did not show any adverse response to EMF exposure at the morphological, photosynthetic, or biochemical level. Variation in the values of the investigated parameters were driven mainly by plants growth and development, and age-dependent physiological metabolic changes with only minor EMF-related differences. The biochemical parameters revealed the most sensitive parameters of the plants.

868 MHz EMF emitted from soil-buried LoRaWAN antennas functions as a mild, transient physiological modulator rather than a stressor. The field accelerated early growth kinetics without enhancing final biomass, left photosynthetic machinery functionally intact, and induced only trait-specific antioxidant adjustments – namely reduced SOD activity in the absence of elevated H_2O_2 or lipid peroxidation – consistent with decreased ROS generation rather than compromised defence. These findings indicate that IoT/LoRa-relevant EMF levels are unlikely to impose adverse effects on maize under the tested conditions.

The antenna matherial and/or presence *per se* was not biologically neutral, introducing measurable morphological and biochemical signals distinct from Control. Coupled with the leaf-age discontinuity on day 28, this constrains the inferential weight of measurements at that time point and highlights the need for full-crop-cycle studies before definitive risk assessments for wireless sensor deployment in precision agriculture can be established.

 doi:10.20944/preprints202605.0378.v1

As low intensity RF-EMF exposure acts as low to moderate abiotic stressor, it may induces mild oxidative stress activating antioxidant systems and repair enzymes, increasing antioxidants and protective osmolites production (proline). Such activation does not result in severe damages but boost defenses and prepare plant organism against further stress – hormesis. Such protective effect may explain the overall better perfomance of EMF plants compared to Sham. An idea for future investigations is to examine combined effects of low level RF-EMF and other, severe environmental factor, such as high temperature or drought in order to test possible general protective effect of RF exposure. Future work would benefit from investigation of RF-EMF effects in real field conditions.

Supplementary Materials: The following supporting information can be downloaded at the website of this paper posted on Preprints.org, Table S1: Plant height raw data; Table S2: Gompertz model parameters; Table S3: Leaf biomass raw data; Table S4: Reducing sugars raw data; Table S5: JIP-test parameters raw data; Table S6: MDA raw data; Table S7: Hidrogen peroxide raw data; Table S8: TEAC raw data; Table S9: SOD activity raw data; Table S10: CAT activity raw data; Table S11: Data used for PCA; Table S12: Correlation coefficients of examined parameters.

Author Contributions: Conceptualization, N.A. and M.K.; methodology, M.P., B.A. and M.K.; software, M.P.; validation, M.P., N.A. and M.K.; formal analysis, M.P. and V.G.; investigation, M.P., B.A. and M.K.; resources, B.N.A., N.A.; data curation, M.P., M.K. and V.G.; writing—original draft preparation, M.P., B.A., B.N.A., N.A., M.K. and V.G.; writing—review and editing, M.P., B.A., B.N.A., N.A., M.K. and V.G.; visualization, M.P. and V.G.; supervision, M.K. and V.G.; project administration, M.P.; funding acquisition, N.A. All authors have read and agreed to the published version of the manuscript.

Funding: This research was funded by the Bulgarian National Science Fund at the Ministry of Education and Science, Bulgaria, grant number KP-06-H67/4, from 12 December 2022: "Development and testing of new models of radio channels and antennas for reliable and resilient wireless connectivity enabling innovative applications in future IoT-based precision agriculture".

Institutional Review Board Statement: Not applicable.

Informed Consent Statement: Not applicable.

Data Availability Statement: The original contributions presented in this study are included in the article/Supplementary Material. Further inquiries can be directed to the corresponding authors.

Acknowledgments: We are thankful to Sonya Goranovska from the Maize Research Institute, Knezha for providing the maize seeds. We are grateful to Alexandra Besheva and Theodora Vlachkova for their invaluable help with the experimental measurements. During the preparation of this manuscript, the authors used Kimi K2.6 (Moonshot AI) and Genspark AI Assistant for the purposes of interpreting the statistical results, drafting and restructuring the Discussion and Conclusions sections, and harmonizing the academic style and language. All data analysis, modelling decisions, and scientific interpretations were performed by the authors, who reviewed, edited, and take full responsibility for the final content of this publication.

Conflicts of Interest: The authors declare no conflicts of interest. The funders had no role in the design of the study; in the collection, analyses, or interpretation of data; in the writing of the manuscript; or in the decision to publish the results.

Abbreviations

The following abbreviations are used in this manuscript:

ANOVA	Analysis of Variance
ATP	Adenosine Triphosphate
CAT	Catalase
DW	Dry Weight
EM	Electromagnetic
EMF	Electromagnetic Field
FW	Fresh Weight

 doi:10.20944/preprints202605.0378.v1

IoT	Internet of Things
LoRa	Long Range telecomunication
MDA	Malondialdehyde
NADPH	Nicotinamide Adenine Dinucleotide Phosphate (reduced form)
PCA	Principal Component Analysis
PI_{total}	Performance Index of the total light-dependent photosynthetic reactions
RF	Radio Frequency
ROS	Reactive Oxygen Species
SEM	Standard Error of Mean
SOD	Superoxide Dismutase
TEAC	Trolox Equivalent Antioxidant Capacity
U	Unit of enzyme activity

References

1. Hardesty, G. IoT Wireless Protocol Selection and Frequency Band Characteristics. The Frequency Bands of IoT Wireless 2024.
2. Elboushi, A.; Telba, A.; Sebak, A.; Jamil, K. Electromagnetic Soil Characterization for Undergrounded RFID System Implementation. *Electronics* **2020**, *9*, 106, doi:10.3390/electronics9010106.
3. Chen, X.; Lü, X.; Zhang, W.; Xue, C.; Zhu, X.; Bao, W. Miniaturized Buried Low-Frequency Acoustically Actuated Magnetoelectric Antenna for Soil Moisture Adaptive Underground Communication. *iScience* **2024**, *27*, doi:10.1016/j.isci.2024.111151.
4. Atanasov, N.T.; Atanasov, B.N.; Atanasova, G.L. Evaluation of Impact of Soil on Performance of Monopole Antenna for IoT Applications in Urban Agriculture. *Electronics* **2025**, *14*, 544, doi:10.3390/electronics14030544.
5. Kouzmanova, M.; Paunov, M.; Angelova, B.; Goltsev, V. From Exposure to Response: Mechanisms of Plant Interaction with Electromagnetic Fields Used in Smart Agriculture. *Appl. Sci.* **2026**, *16*, doi:10.3390/app16010370.
6. Pal, A.; Batish, D.R.; Kaur, S.; Singh, R. Investigating the Long–Term Exposure Effects of 2850 MHz EMF-r on Growth, Physiology and Carbohydrate Metabolism of Triticum Aestivum L. *Curr. Agric. Res. J.* **2024**, *12*.
7. Tang, C.; Yang, C.; Yu, H.; Tian, S.; Huang, X.; Wang, W.; Cai, P. Electromagnetic Radiation Disturbed the Photosynthesis of Microcystis Aeruginosa at the Proteomics Level. *Sci. Rep.* **2018**, *8*, 479, doi:10.1038/s41598-017-18953-z.
8. Halgamuge, M.N. Review: Weak Radiofrequency Radiation Exposure from Mobile Phone Radiation on Plants. *Electromagn. Biol. Med.* **2017**, *36*, 213–235, doi:10.1080/15368378.2016.1220389.
9. Tran, N.T.; Jokic, L.; Keller, J.; Geier, J.U.; Kaldenhoff, R. Impacts of Radio-Frequency Electromagnetic Field (RF-EMF) on Lettuce (Lactuca Sativa)—Evidence for RF-EMF Interference with Plant Stress Responses. *Plants* **2023**, *12*, doi:10.3390/plants12051082.
10. Gustavino, B.; Carboni, G.; Petrillo, R.; Paoluzzi, G.; Santovetti, E.; Rizzoni, M. Exposure to 915 MHz Radiation Induces Micronuclei in Vicia Faba Root Tips. *Mutagenesis* **2016**, *31*, 187–192, doi:10.1093/mutage/gev071.
11. Vian, A.; Davies, E.; Gendraud, M.; Bonnet, P. Plant Responses to High Frequency Electromagnetic Fields. *BioMed Res. Int.* **2016**, *2016*, 1830262.
12. Stefi, A.L.; Margaritis, L.H.; Christodoulakis, N.S. The Effect of the Non Ionizing Radiation on Cultivated Plants of *Arabidopsis Thaliana* (Col.). *Flora* **2016**, *223*, 114–120, doi:10.1016/j.flora.2016.05.008.
13. Kumar, A.; Kaur, S.; Chandel, S.; Singh, H.P.; Batish, D.R.; Kohli, R.K. Comparative Cyto- and Genotoxicity of 900 MHz and 1800 MHz Electromagnetic Field Radiations in Root Meristems of Allium Cepa. *Ecotoxicol. Environ. Saf.* **2020**, *188*, 109786.
14. Tkalec, M.; Malarić, K.; Pevalek-Kozlina, B. Influence of 400, 900, and 1900 MHz Electromagnetic Fields on *Lemna Minor* Growth and Peroxidase Activity. *Bioelectromagnetics* **2005**, *26*, 185–193, doi:10.1002/bem.20104.
15. Roux, D.; Vian, A.; Girard, S.; Bonnet, P.; Paladian, F.; Davies, E.; Ledoigt, G. High Frequency (900 MHz) Low Amplitude (5 V M−1) Electromagnetic Field: A Genuine Environmental Stimulus That Affects

 doi:10.20944/preprints202605.0378.v1

Transcription, Translation, Calcium and Energy Charge in Tomato. *Planta* **2008**, *227*, 883–891, doi:10.1007/s00425-007-0664-2.

16. Karipidis, K.; Brzozek, C.; Mate, R.; Bhatt, C.R.; Loughran, S.; Wood, A.W. What Evidence Exists on the Impact of Anthropogenic Radiofrequency Electromagnetic Fields on Animals and Plants in the Environment: A Systematic Map. *Environ. Evid.* **2023**, *12*, 9, doi:10.1186/s13750-023-00304-3.
17. Kaur, S.; Vian, A.; Chandel, S.; Singh, H.P.; Batish, D.R.; Kohli, R.K. Sensitivity of Plants to High Frequency Electromagnetic Radiation: Cellular Mechanisms and Morphological Changes. *Rev. Environ. Sci. Biotechnol.* **2021**, *20*, 55–74, doi:10.1007/s11157-020-09563-9.
18. Racuciu, M.; Iftode, C.; Miclaus, S. Inhibitory Effects of Low Thermal Radiofrequency Radiation on Physiological Parameters of Zea Mays Seedlings Growth. *Romanian J. Phys.* **2015**, *60*, 603–612.
19. Sharma, V.P.; Singh, H.P.; Kohli, R.K.; Batish, D.R. Mobile Phone Radiation Inhibits *Vigna Radiata* (Mung Bean) Root Growth by Inducing Oxidative Stress. *Sci. Total Environ.* **2009**, *407*, 5543–5547, doi:10.1016/j.scitotenv.2009.07.006.
20. Moiroux-Arvis, L.; Cariou, C.; Chanet, J.-P. Evaluation of LoRa Technology in 433-MHz and 868-MHz for Underground to Aboveground Data Transmission. *Comput. Electron. Agric.* **2022**, *194*, 106770, doi:10.1016/j.compag.2022.106770.
21. Strasser, R.J.; Tsimilli-Michael, M.; Srivastava, A. Analysis of the Chlorophyll *a* Fluorescence Transient. In *Chlorophyll* a *Fluorescence: a Signature of Photosynthesis*; Papageorgiou, G., Govindjee, Eds.; Advances in Photosynthesis and Respiration; Springer: Dordrecht, The Netherlands, 2004; pp. 321–362.
22. Strasser, R.J.; Tsimilli-Michael, M.; Qiang, S.; Goltsev, V. Simultaneous *in Vivo* Recording of Prompt and Delayed Fluorescence and 820-Nm Reflection Changes during Drying and after Rehydration of the Resurrection Plant *Haberlea Rhodopensis*. *Biochim Biophys Acta* **2010**, *1797*, 1313–1326.
23. Plummer, D.T. *An Introduction to Practical Biochemistry*; McGraw-Hill Book Company London, 1987; ISBN 0-07-084165-9.
24. López-Hidalgo, C.; Meijón, M.; Lamelas, L.; Valledor, L. The Rainbow Protocol: A Sequential Method for Quantifying Pigments, Sugars, Free Amino Acids, Phenolics, Flavonoids and MDA from a Small Amount of Sample; Wiley Online Library, 2021;
25. Re, R.; Pellegrini, N.; Proteggente, A.; Pannala, A.; Yang, M.; Rice-Evans, C. Antioxidant Activity Applying an Improved ABTS Radical Cation Decolorization Assay. *Free Radic. Biol. Med.* **1999**, *26*, 1231–1237.
26. Kouzmanova, M.; Angelova, B.; Atanasova, G.; Atanasov, B.; Atanasov, N.; Goltsev, V.; Paunov, M. Electromagnetic Fields in Precision Agriculture: Do They Provoke Oxidative Stress in Maize Plants? *Bulg. J. Agric. Sci.* **2024**, *30*.
27. Aebi, H. Catalase in Vitro. In *Methods in enzymology*; Elsevier, 1984; Vol. 105, pp. 121–126 ISBN 0076-6879.
28. SOD Assay Kit Sufficient for 500 Tests Superoxide Dismutase Assay Kit Available online: https://www.sigmaaldrich.com/BG/en/product/sigma/19160 (accessed on 4 May 2026).
29. Experimental Data Analysis / Two-Way ANOVA in R · GitLab Available online: https://gitlab.com/experimental-data-analysis/two-way-anova-in-r (accessed on 2 May 2026).
30. Kumar, A.; Singh, H.P.; Batish, D.R.; Kaur, S.; Kohli, R.K. EMF Radiations (1800 MHz)-Inhibited Early Seedling Growth of Maize (Zea Mays) Involves Alterations in Starch and Sucrose Metabolism. *Protoplasma* **2016**, *253*, 1043–1049, doi:10.1007/s00709-015-0863-9.
31. Zareh, H.; Mohsenzadeh, S. Electromagnetic Waves from GSM Mobile Phone Simulator Increase Germination and Abiotic Stress in Zea Mays L. **2015**.
32. Paunov, M.; Angelova, B.; Goltsev, V.; Atanasova, G.; Atanasov, B.; Atanasov, N.; Kouzmanova, M. Electromagnetic Field Used in Precision Agriculture Does Not Induce Long-Term Effects in Wheat and Maize. *Proc. Bulg. Acad. Sci.* **2025**, *78*, 1083–1093, doi:10.7546/CRABS.2025.07.15.
33. Brestic, M.; Strasser, R.; Goltsev, V. In Vivo Measurements of Light Emission in Plants. *Photosynth. Open Quest. What We Know Today Allakhverdiev SI Rubin AB Shuvalov VA Eds* **2014**.
34. Roux, D.; Catrain, A.; Lallechere, S.; Joly, J.-C. Sunflower Exposed to High-Intensity Microwave-Frequency Electromagnetic Field: Electrophysiological Response Requires a Mechanical Injury to Initiate. *Plant Signal. Behav.* **2015**, *10*, e972787.

 doi:10.20944/preprints202605.0378.v1

35. Senavirathna, M.; Asaeda, T. Radio-Frequency Electromagnetic Radiation Alters the Electric Potential of Myriophyllum Aquaticum. *Biol. Plant.* **2014**, *58*, 355–362.
36. Majeran, W.; Friso, G.; Ponnala, L.; Connolly, B.; Huang, M.; Reidel, E.; Zhang, C.; Asakura, Y.; Bhuiyan, N.H.; Sun, Q.; et al. Structural and Metabolic Transitions of C4 Leaf Development and Differentiation Defined by Microscopy and Quantitative Proteomics in Maize. *Plant Cell* **2010**, *22*, 3509–3542, doi:10.1105/tpc.110.079764.
37. Abdollahi, F.; Niknam, V.; Ghanati, F.; Masroor, F.; Noorbakhsh, S.N. Biological Effects of Weak Electromagnetic Field on Healthy and Infected Lime (Citrus Aurantifolia) Trees with Phytoplasma. *Sci. World J.* **2012**, *2012*, 716929.
38. Großkinsky, D.K.; Syaifullah, S.J.; Roitsch, T. Integration of Multi-Omics Techniques and Physiological Phenotyping within a Holistic Phenomics Approach to Study Senescence in Model and Crop Plants. *J. Exp. Bot.* **2018**, *69*, 825–844, doi:10.1093/jxb/erx333.
39. Tucker, S.L.; Dohleman, F.G.; Grapov, D.; Flagel, L.; Yang, S.; Wegener, K.M.; Kosola, K.; Swarup, S.; Rapp, R.A.; Bedair, M.; et al. Evaluating Maize Phenotypic Variance, Heritability, and Yield Relationships at Multiple Biological Scales across Agronomically Relevant Environments. *Plant Cell Environ.* **2020**, *43*, 880–902, doi:10.1111/pce.13681.
40. Seebacher, F.; Little, A.G. Mechanisms Underlying Phenotypic Plasticity in Response to Environmental Change. *Biol. Rev.* **2026**, *101*, 713–734, doi:10.1111/brv.70100.
41. Sultan, S.E. Phenotypic Plasticity for Plant Development, Function and Life History. *Trends Plant Sci.* **2000**, *5*, 537–542, doi:10.1016/S1360-1385(00)01797-0.
42. Nicotra, A.B.; Atkin, O.K.; Bonser, S.P.; Davidson, A.M.; Finnegan, E.J.; Mathesius, U.; Poot, P.; Purugganan, M.D.; Richards, C.L.; Valladares, F.; et al. Plant Phenotypic Plasticity in a Changing Climate. *Trends Plant Sci.* **2010**, *15*, 684–692, doi:10.1016/j.tplants.2010.09.008.